The Plant Cell, Vol. 15, 2093–2105, September 2003, www.plantcell.org © 2003 American Society of Plant Biologists

Endoreduplication Mediated by the Anaphase-Promoting Complex Activator CCS52A Is Required for Symbiotic Cell Differentiation in *Medicago truncatula* Nodules

Jose Maria Vinardell,[1] Elena Fedorova,[2] Angel Cebolla,[3] Zoltan Kevei,[4] Gabor Horvath,[4] Zsolt Kelemen, Sylvie Tarayre, François Roudier,[5] Peter Mergaert, Adam Kondorosi, and Eva Kondorosi[6]

Institut des Sciences du Végétal, Centre National de la Recherche Scientifique Unité Propre de Recherche 2355, 91198 Gif-sur-Yvette, France

In *Medicago* nodules, endoreduplication cycles and ploidy-dependent cell enlargement occur during the differentiation of bacteroid-containing nitrogen-fixing symbiotic cells. These events are accompanied by the expression of *ccs52A*, a plant ortholog of the yeast and animal *cdh1*/*srw1*/*fzr* genes, acting as a substrate-specific activator of the anaphase-promoting complex (APC) ubiquitin ligase. Because CCS52A is involved in the transition of mitotic cycles to endoreduplication cycles, we investigated the importance of somatic endoploidy and the role of the *M. truncatula ccs52A* gene in symbiotic cell differentiation. Transcription analysis and *ccs52A* promoter–driven β-glucuronidase activity in transgenic plants showed that *ccs52A* was dispensable for the mitotic cycles and nodule primordium formation, whereas it was induced before nodule differentiation. The CCS52A protein was present in the nucleus of endoreduplication-competent cells, indicating that it may activate APC constitutively during the endoreduplication cycles. Downregulation of *ccs52A* in transgenic *M. truncatula* plants drastically affected nodule development, resulting in lower ploidy, reduced cell size, inefficient invasion, and the maturation of symbiotic cells, accompanied by early senescence and finally the death of both the bacterium and plant cells. Thus, *ccs52A* expression is essential for the formation of large highly polyploid symbiotic cells, and endoreduplication is an integral part of normal nodule development.

INTRODUCTION

Somatic endoploidy is widespread in plants in which most cell types can support one or several rounds of endoreduplication (duplication of the genome without mitosis) (Nagl, 1978). The inherited pattern of endoploidy, which is characteristic of the different organs in a given species, suggests that multiplication of the genome might contribute to the differentiation of certain cell types. Our knowledge of the role of endoreduplication is still rudimentary; however, a direct relationship between DNA content and cell size in endoreplicative tissues indicates that an increased genome size may be required for the formation of large plant cells (Kondorosi et al., 2000). Moreover, the absence of chromosome condensation and an increase in gene dosage can explain the greater transcriptional and metabolic activities of polyploid cells, and as in yeast (Galitski et al., 1999), the ploidy-dependent expression of a subset of the genome might control and specify cell functions.

The diploid model legume *Medicago truncatula* exhibits various degrees of endoploidy in all organs except leaves. The highest level of somatic endoploidy was measured in nitrogen-fixing root nodules that are formed in symbiosis with the soil bacterium *Sinorhizobium meliloti*. Nodule organogenesis is induced in the absence of combined nitrogen by *S. meliloti* nodulation (Nod) factors that activate the cell cycle in G0-arrested cortical cells, leading to cell division in the inner cortex and the initiation of the nodule primordium, which after its outgrowth of the root differentiates into various nodule cell types (Vasse et al., 1990; Foucher and Kondorosi, 2000). The central region of a mature nitrogen-fixing nodule is composed of the persistent apical meristem (zone I), the infection zone II, the nitrogen fixation zone III, and, in old nodules, a proximal senescent zone IV. Infection of plant cells and differentiation of symbiotic cells occur in zone II. In this zone, the bacteria still produce Nod factors, and although the cells do not divide, they are able to undergo successive rounds of endoreduplication cycles composed of G1-S-G2 phases. As a consequence, the nuclear DNA content increases from 2C up to 64C, and, proportional to the genome size, the cells enlarge drastically as they become older and more distant from the meristem during longitudinal nodule growth (Truchet, 1978; Cebolla et al., 1999). In the infected cells, each bacterium surrounded by a peribacteroid membrane forms a symbiosome. These membrane-encapsulated bacteria, named bacteroids, first multiply and then grow

[1] Current address: Departamento de Microbiologia, Facultad de Biologia, Universidad de Sevilla, Avda. Reina Mercedes 6, 41012 Sevilla, Spain.
[2] Current address: Timiriazev Institute of Plant Physiology, Russian Academy of Sciences, Botanicheskaya 35, Moscow 127276, Russia.
[3] Current address: Biomedal SL Centro de Empresas Pabellón de Italia, Planta 3ª, Sector NO, Avda. Isaac Newton, sn. Isla de la Cartuja, 41092 Sevilla, Spain.
[4] Current address: Biological Research Center of the Hungarian Academy of Sciences, 6726 Szeged, Temesvari krt. 62, Hungary.
[5] Current address: Duke University, DCMB-LSRC, 104 Research Drive, Durham, NC 27708.
[6] To whom correspondence should be addressed. E-mail eva.kondorosi@isv.cnrs-gif.fr; fax 33-1-69-82-36-95.
Article, publication date, and citation information can be found at www.plantcell.org/cgi/doi/10.1105/tpc.014373.

and mature simultaneously with the endoreduplicating host cell. In zone III, the differentiation of both plant and bacterial cells is terminated: there is no Nod factor production, the expression of cell cycle genes is switched off, and the symbiotic cells are at their final size and are fully packed with extremely enlarged, elongated, nitrogen-fixing bacteroids.

Recently, we identified the cell cycle switch gene *ccs52* from an alfalfa (*Medicago sativa*) nodule cDNA library. Overexpression of this gene in fission yeast resulted in the degradation of the mitotic cyclin Cdc13, which provoked division arrest, induction of endoreduplication cycles, and the formation of large, elongated yeast cells (Cebolla et al., 1999). In planta, expression of *ccs52* was linked to cell differentiation and endoreduplication. In the nitrogen-fixing nodules, the *ccs52* transcripts were localized in zone I, where cells exit constantly from the mitotic cycle, and in zone II, where endoreduplication occurs, whereas the transcripts were not detected in zone III and in peripheral nodule tissues (Cebolla et al., 1999).

CCS52 belongs to a WD40-repeat protein family whose members act as substrate-specific activators of the anaphase-promoting complex (APC), a cell cycle–regulated E3 ubiquitin ligase (reviewed by Vodermaier, 2001) whose activity increases from metaphase to anaphase and remains high throughout G1, then decreases in S/G2 (Fang et al., 1998). In the absence of these WD40-repeat proteins, APC has little ubiquitin ligase activity. The activators play dual roles: by their binding, they activate the APC in the nucleus and select distinct proteins for degradation by the 26S proteasome (Visintin et al., 1997; Fang et al., 1998; Pfleger et al., 2001). This protein family can be divided into two groups, the CDC20/FZY and CDH1/SRW1(STE9)/FZR subfamilies, which show differences in their substrate recognition motifs and in the timing of APC activation. CCS52 belongs to the latter subfamily (Cebolla et al., 1999). APC activators from both groups are able to recruit proteins containing the destruction box (D box; RXXL sequence) (Glotzer et al., 1991) that was first identified in the animal A- and B-type mitotic cyclins whose controlled production and degradation are essential for the regulation of cyclin-dependent kinase activities during the G2/M transition and the M-phase progression. In addition, the CDH1-type proteins can recognize and elicit the degradation of KEN box–containing (Pfleger and Kirschner, 2000) and A box–containing (Littlepage and Ruderman, 2002) substrates.

Plants possess particularly high numbers and variants of mitotic cyclins. The Arabidopsis genome contains 10 A-type and 9 B-type cyclins (Vandepoele et al., 2002), and similar complexity of mitotic cyclins is expected in other plant species. It is largely unknown how all of these mitotic cyclins function in the cell cycle and when they are degraded. The D box destruction pathway also exists in plants (Genschik et al., 1998), and our previous results showed that CCS52 was able to target the degradation of mitotic cyclins (Cebolla et al., 1999). Based on these data and the known functions of APC activators, it is likely that CCS52 controls endoreduplication in plant cells by the altered degradation of mitotic cyclins compared with mitotic cycles, which provokes M-phase inhibition and the conversion of the mitotic cell cycle to endoreduplication cycles (or endocycles).

Here, we analyzed the role of *ccs52* and the significance of somatic endoploidy in nodule development. Previously, we showed that plants have multiple *ccs52* homologs (Cebolla et al., 1999). We report on the isolation and characterization of *Mtccs52A*, the nodule-expressed form of the *ccs52* gene family from *M. truncatula*, and show that this gene is not required for cell proliferation during the establishment of a nodule primordium but is essential for the differentiation of the large polyploid symbiotic cells. Moreover, immunolocalization of CCS52A in nodule sections indicates that CCS52A might provide nonperiodic APC activity during endoreduplication cycles, in contrast to the M-G1–phase functions of APC during mitotic cycles.

RESULTS

The *ccs52* Gene Structure

The *ccs52A* cDNA as well as its genomic clone were isolated from the diploid, autogamous *M. truncatula*. The *Mtccs52A* cDNA obtained from a nodule cDNA library encodes a 475–amino acid, 52,457-D protein (pI = 8.86) that exhibits 99.6% identity to CCS52, which was identified previously from *M. sativa* nodules (renamed MsCCS52A), differing at positions 16 (G_{Mt}/R_{Ms}) and 141 (I_{Mt}/V_{Ms}). The *Mtccs52A* gene was localized on a 9.6-kb EcoRI genomic DNA fragment. Alignment of the sequenced 8450-bp genomic region with the *Mtccs52A* cDNA revealed that the *Mtccs52A* gene comprises 10 exons and 9 introns (Figure 1). A potential TATA box and a transcriptional start site were predicted at positions 2246 and 2276 ($\pm$10), respectively, and exon 1, starting at position 2461, encoded the entire N-terminal region (158 amino acids) in front of the WD40 repeats (Figure 1).

Mtccs52A Is Activated at the Final Stage of Primordium Formation before the Differentiation of Nodule Zones

Previously, by RNA gel blot analysis and in situ hybridization, we showed the presence of *ccs52* transcripts in all organs of *M. sativa* at varying levels (Cebolla et al., 1999). However, the recent isolation of the *ccs52B* gene (J.M. Vinardell and S. Tarayre, unpublished data) revealed that these hybridizations with the full-length *ccs52A* cDNA did not distinguish the A- and B-type members of the family. Therefore, to study specifically the expression pattern of *Mtccs52A*, its promoter region (Figure 1) was cloned in a binary vector containing the promoterless *uidA* reporter gene encoding β-glucuronidase (GUS). The resulting plasmid, pISV2613, was introduced into *Agrobacterium tumefaciens* to transform *M. truncatula*. In seven independent transgenic lines from the T0 to T2 generations, the *Mtccs52A* promoter–driven GUS activity was monitored during nodule development (Figure 2).

Unlike many cell cycle genes, such as histone H3, *cycB2;3*, and *cycA2;2*, that are induced from the onset of nodule organogenesis (Foucher and Kondorosi, 2000; Roudier et al., 2003), in the *ccs52A* promoter-GUS lines no GUS activity was detected in the dividing cortical cells (Figure 2A, arrows) or in the emerging, growing nodule primordia (Figure 2B, black arrows), indicating that *ccs52A* expression is not required for cell prolif-

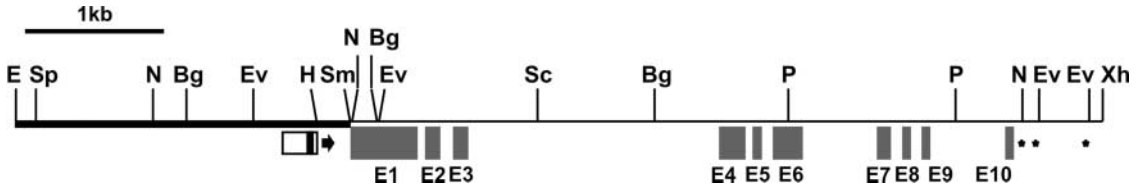

Figure 1. Organization of the *M. truncatula Mtccs52A* Gene.

Restriction map of the sequenced 8450-bp region. The putative promoter sequence is shown as a white rectangle, with the TATA box shown in black. The arrow indicates the potential transcriptional start site. Exons (E1 to E10) are represented by gray boxes, and polyadenylation sites are represented by stars. The 2436-bp EcoRI-SmaI fragment used for *uidA* expression in transgenic *M. truncatula* plants is indicated by the boldface line. Bg, BglII; E, EcoRI; Ev, EcoRV; H, HindIII; N, NcoI; P, PstI; Sc, SacI; Sm, SmaI; Sp, SphI; Xh, XhoI.

eration. Expression of *Mtccs52A* was switched on before nodule differentiation in the central region of fully grown primordia (Figures 2B, red arrows, and 2C). With nodule differentiation, GUS staining was observed in nodule zones I and II but not in the nitrogen-fixing zone (Figure 2D). This expression profile was maintained in mature, elongated nodules (Figure 2E) and was consistent with the in situ localization of the *ccs52A* transcripts in nodule zones I and II (Cebolla et al., 1999).

The *Mtccs52A* promoter–driven GUS activity was confirmed by semiquantitative reverse transcriptase–mediated (RT) PCR experiments (Figure 3A). RNA was isolated from the nodulation-competent zone of uninoculated roots (stage A), from *S. meliloti*–inoculated root segments at 1 and 2 days after inoculation, corresponding to the initial stage of nodule development when the first cortical cell divisions occur (stage B), from young growing primordia at 3 and 4 days after inoculation (stage C), from differentiating primordia (5 days after inoculation) and young nitrogen-fixing nodules at 7 days after inoculation (stage D), and from nitrogen-fixing nodules (stage E) from 10 to 28 days after inoculation. The RNA concentration of the samples was quantified by RT-PCR analysis of the constitutive control gene *c27* (Györgyey et al., 1991). In these samples, the expression of *ccs52A*, *ccs52B*, and *enod40*, an early nodule-specific nodulin gene (Crespi et al., 1994), all normalized with the expression of *c27*, was studied (Györgyey et al., 1991). Although *enod40* was induced already in developmental stage B at 2 days after inoculation, when cell proliferation starts, *ccs52A* was activated in stage D in fully grown nodule primordia (5 days after inoculation), and its expression was maximal at the conversion of nodule primordia to nitrogen-fixing nodules (7 days after inoculation). This delayed expression and the lack of *ccs52A* activation in proliferating primordium cells were consistent with the involvement of CCS52A in M-phase inhibition and proliferation arrest. These RT-PCR experiments as well as RNA gel blot hybridizations (data not shown) also revealed that the expression of *ccs52A* was significantly weaker than that of *enod40*. Correspondingly, in the TIGR *M. truncatula* Gene Index (http://www.tigr.org/tdb/tgi/mtgi/), *enod40* is represented by 31 ESTs, whereas *ccs52A* is represented by only a single EST in the nodule libraries.

Unlike *ccs52A*, the *ccs52B* gene was expressed in the root and in inoculated root segments in stages B and C. However, as soon as the nodule primordium appeared and could be separated from the root, *ccs52B* transcript levels decreased (stage D), and they were practically absent in the differentiating nitrogen-fixing nodules (E). In accordance with this finding, *ccs52B* could not be amplified from our young nodule cDNA library but could be isolated from a root library. Moreover, none of the five *ccs52B* ESTs present in the TIGR *M. truncatula* Gene Index was derived from nodule libraries. Therefore, *ccs52A* might be the only member of the family that is expressed during the differentiation of nitrogen-fixing nodules.

CCS52A May Activate APC Constitutively in Endoreduplication-Competent Cells

The functions of APC are unexplored in plants. In yeast and animals, APC is studied predominantly in the cell cycle, and although the core APC components also are present in postmitotic cells (e.g., terminally differentiated neurons) (Gieffers et al., 1999), the role of APC outside of the cell cycle, including the endoreduplication cycle, is largely unstudied (reviewed by Harper et al., 2002). Because endoreduplication is particularly important for plant development and requires CCS52A, we monitored APC activities based on the presence and localization of this APC activator in endoreduplicating nodule cells.

The *ccs52A* promoter–driven GUS activity (Figure 2E) and the in situ hybridization of *ccs52A* (Cebolla et al., 1999) showed that *ccs52A* was expressed in the entire nodule zone II. This homogenous expression of *ccs52A* was different from that of cell cycle–regulated genes such as the S-phase–specific histone H3, which give patchy expression patterns (Figure 2F, black spots). Therefore, the cell cycle might not affect or might only weakly affect *ccs52A* expression, whereas cell cycle regulation of the CCS52A protein cannot be excluded.

CCS52A contains a PEST degradation motif that can affect protein stability as well as six phosphorylation sites, which in the orthologous yeast and animal CDH1 proteins regulate both the CDH1–APC interaction (Zachariae et al., 1998) and the intracellular localization of the protein that is nuclear in its active, hypophosphorylated form (Jaquenoud et al., 2002; Zhou et al., 2003). The immunolocalization of CCS52A was performed in nodule sections using polyclonal antibodies raised against the *M. truncatula* CCS52A protein that reacted specifically with CCS52A but not with CCS52B. CCS52A was detected by the green signal of the fluorescein isothiocyanate–conjugated sec-

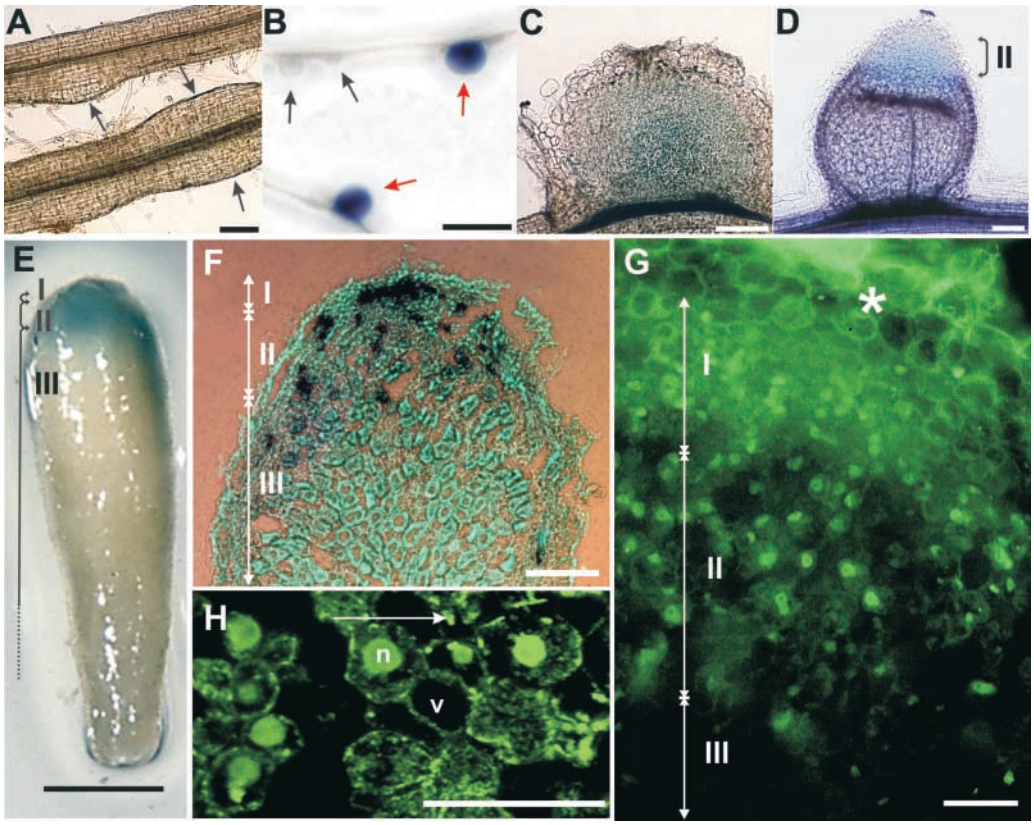

Figure 2. Expression of *Mtccs52A* during Nodule Development.

(A) to **(E)** GUS staining in transgenic *M. truncatula* plants harboring the *Mtccs52A* promoter–*uidA* fusion.
(A) Formation of the de novo nodule meristems (arrows) in the root cortex.
(B) Emerging (black arrows) and mature (red arrows) nodule primordia.
(C) GUS staining in the central region of the nodule primordium.
(D) A young differentiating nodule.
(E) Mature nitrogen-fixing nodules with elongated zone III.
(F) Spotty expression of histone H3 detected by in situ hybridization.
(G) Immunolocalization of the CCS52A protein in nodule zones I and II. The asterisk indicates the nodule cortex.
(H) Confocal image of zone-II cells. The arrow indicates the maturation of nodule cells from younger to older stages.
Roman numerals indicate the nodule zones. n, nucleus; v, vacuole. Bars = 0.2 mm in **(A)**, **(D)**, and **(F)**, 0.25 mm in **(C)**, 1 mm in **(B)** and **(F)**, and 10 μm in **(G)** and **(H)**.

ondary antibodies. Although there was a nonspecific background signal in the nodule periphery, where cells did not express *ccs52A*, the protein clearly was present in nodule zones I and II and localized predominantly in the nuclei (Figure 2G). As a result of differences in cell size, the nodule sections contained several cell layers of the meristem and only a single layer at the distal part of zone II. Therefore, it was difficult to quantify in the meristem how many cells contained CCS52A, whereas the protein was present in all zone-II cells. As shown by confocal microscopy of zone II (Figure 2H), CCS52A was overwhelmingly abundant in the nuclei. In cells in which the nuclear signal was absent, the confocal image plane was through the vacuole and not through the nucleus. The nuclear localization of CCS52A indicates that the protein is present in its active form in zone-II cells, which suggests that CCS52A might provide constitutive APC activity in postmitotic cells undergoing endoreduplication cycles.

Expression of *ccs52A* Correlates with the Development of Polyploid Nodule Cells

Flow cytometry was used to test how somatic ploidy evolved during nodule development and how the appearance of polyploid cell populations correlated with the transcript levels of *ccs52A* (Figure 3B). The nuclear DNA content of cells was measured in the nodulation-competent zone of uninoculated roots (stage A), in fully grown and differentiating nodule primordia (stage D), and in mature but still growing nitrogen-fixing nodules (stage E). Because the 4C DNA content may correspond to G2-arrested cells, only nuclei with ≥8C DNA were considered

to have resulted from endoreduplication cycles. In the uninoculated root segment (stage A), >95% of the cells contained 2C to 4C nuclei, and endoreduplication resulting in 8C cells occurred in <4% of the cells. In stage D, 22% of the nuclei were endoreduplicated. The percentage of polyploid cells increased further during nodule maturation (stage E), and nodules that were 2 mm long at 15 days after inoculation contained ~40% polyploid cells. Because the DNA content of proliferating primordium cells is 2C or 4C, the appearance of ≥8C in the differentiating young nodules (stage D) is consistent with the activation and predicted function of *ccs52A* in cell cycle exit and endoreduplication.

Downregulation of *ccs52A* Expression Decreases the Ploidy Level and Inhibits the Development of Nitrogen-Fixing Nodules

In our previous work, *M. truncatula* was transformed with the *ccs52A* cDNA that was expressed in the sense and antisense orientations from the 35S promoter of *Cauliflower mosaic virus* (Cebolla et al., 1999). Because none of the sense plants exhibited overexpression of the transgene, the transformation was repeated using the 35S promoter with double enhancer for *ccs52A* expression. However, again, none of the transgenic plants showed overexpression of *ccs52A*, suggesting that increased levels of CCS52A may interfere with somatic embryogenesis by inhibiting cell proliferation and proembryogenic callus formation. Therefore, the regeneration of plants might be possible only if transgene expression is silenced. To avoid the expression of *ccs52A* during somatic embryogenesis, *ccs52A* cDNA was cloned under the control of two nodule-specific promoters: *enod12* and leghemoglobin. Unexpectedly, transformation of *M. truncatula* with these constructs resulted in only a few (seven and five, respectively) transgenic plants without overexpression of *ccs52A*, because these promoters also were activated during proembryogenic callus formation, probably as a result of the presence of plant hormones in the medium (J.M. Vinardell and E. Kondorosi, unpublished data). With the anti-

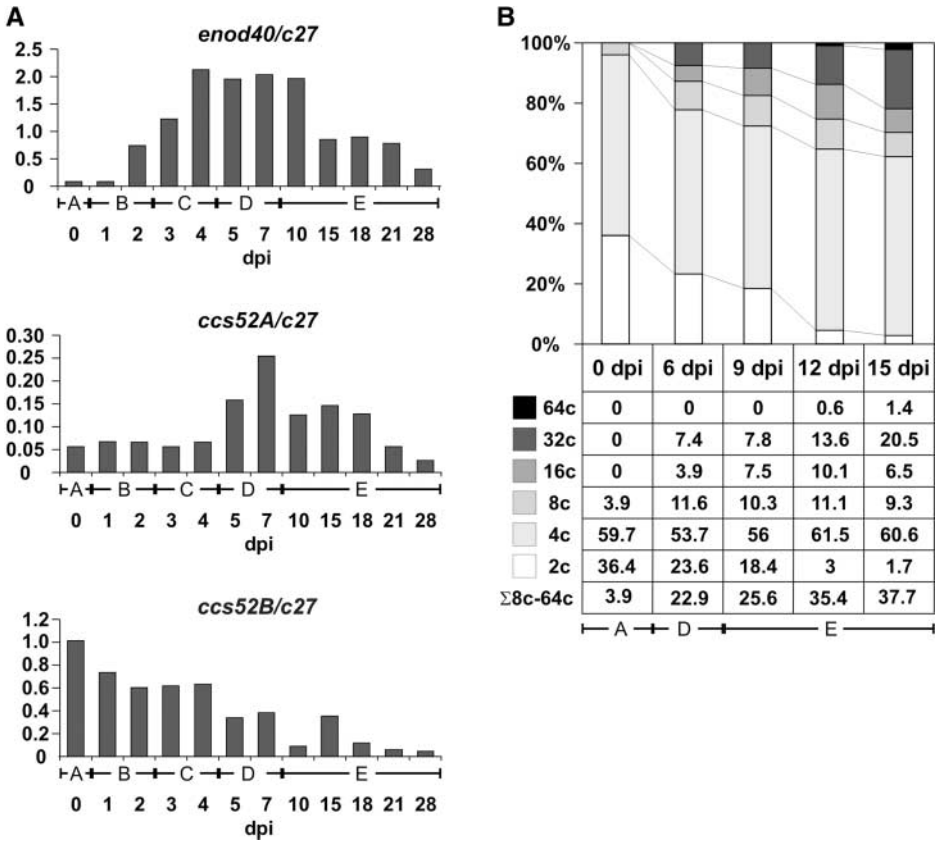

	0 dpi	6 dpi	9 dpi	12 dpi	15 dpi
64c	0	0	0	0.6	1.4
32c	0	7.4	7.8	13.6	20.5
16c	0	3.9	7.5	10.1	6.5
8c	3.9	11.6	10.3	11.1	9.3
4c	59.7	53.7	56	61.5	60.6
2c	36.4	23.6	18.4	3	1.7
Σ8c-64c	3.9	22.9	25.6	35.4	37.7

Figure 3. Activation of *ccs52A* Correlates with Nodule Differentiation and the Appearance of Polyploid Cell Populations.

(A) RT-PCR analysis of *enod40*, *ccs52A*, and *ccs52B* expression in the root and at different stages of nodule development after normalization with the constitutive *c27* signal.

(B) Analysis of nuclear DNA content by flow cytometry at different stages of nodule development.

The letters under the bars represent developmental stages as follows: A, nodulation-competent zone of uninoculated root; B, nodule initiation, cortical cell division; C, nodule primordium formation; D, differentiation of the primordium to a nitrogen-fixing nodule; E, nitrogen-fixing nodules at different ages. dpi, days after inoculation.

sense approach, plants with reduced *ccs52A* transcript levels were obtained, but no real knockout plants were produced. The incapacity for overexpressing or silencing *ccs52A* and the low expression of this gene in wild-type plants suggest that modulation of *ccs52A* transcript levels might be possible only within a narrow window.

The effect of antisense *ccs52A* expression on nodulation was studied in the T2 and T3 generations of the A4 transgenic line, which was affected most severely in *ccs52A* expression (Cebolla et al., 1999). These plants as well as control transgenic plants, which were transformed with the same vector but without *ccs52A*, were cultivated in perlite and in aeroponic "nodule factories" in nitrogen-limited nutrient solution (see Methods). Nodulation assays under these two different growth conditions gave similar results. All control plants formed nitrogen-fixing nodules that were elongated and pink as a result of the presence of leghemoglobin, a marker for efficient nitrogen fixation (Figure 4A). In antisense plants, 13 of 58 perlite-grown plants and 12 of 27 factory-grown plants had no nitrogen-fixing nodules. Although the nodule primordia developed normally (Figure 4B, red arrows), the nodules remained small and round (Figures 4B and 4C), and their brown color indicated early senescence. Compared with the control nodules (Figure 4D), these nodules were invaded inefficiently, zone III was absent, and although the meristem was present at the early stage (Figure 4E), it later disappeared (Figure 4F). These plants displayed reduced growth capacities in the absence of combined nitrogen, but their capacities were restored when the plants were cultivated with combined nitrogen (nitrate and ammonium).

To confirm in independent plant lines that aborted nodule development was linked to the downregulation of the *ccs52A* gene, transgenic hairy roots were produced on wild-type *M. truncatula* R108 plants by *Agrobacterium rhizogenes*–mediated transformation. These hairy roots develop directly from primary roots without affecting other organs (Boisson-Dernier et al., 2001). Nodulation of the control hairy root plants was indistinguishable from that of wild-type plants: the nodules were elongated and pink (Figure 4G). By contrast, 5 of 18 *ccs52A* antisense hairy root plants produced only aborted globular nodules or only slightly elongated nodules, which were initially white but then rapidly became brownish (Figure 4H). The absence of pink nodules indicated that these plants, like those of the A4 line, were unable to fix nitrogen; this finding correlated with symptoms of nitrogen starvation in the aerial parts, such as yellow leaf color and reduced green mass (Figure 4I).

The aeroponic growth system allowed continuous observation of the root system to follow the timing of nodule necrosis by the appearance of dark color. At the beginning of nodule development, as in the A4 line, no difference was detected between the control and antisense plants in the structure (Figure 4J) or the number and position of nodule primordia. However, when most primordia developed into nitrogen-fixing nodules in the control plants, senescence had started already in the globular, primordium-like antisense nodules, which were unable to differentiate, and hypertrophy of the peripheral cell layers often was observed (Figure 4K), as in A4 nodules (Figure 4F). Some antisense nodules developed somewhat further and were elongated, but their structures (Figure 4L) were different from those of wild-type nodules (Figure 4M), because the nitrogen fixation zone was absent and necrotic cells were present all over the central region. By contrast, in wild-type nodules, senescence started several weeks later and only at the nodule base (Vasse et al., 1990).

In the aborted antisense nodules, RNA gel blot analysis revealed reduced expression of *ccs52A* (Figure 5A), and protein gel blot analysis revealed a drastic decrease in the CCS52A protein level, which was as weak as the signal in the growing wild-type nodule primordium (Figure 5B). This decrease concerned specifically CCS52A, because the amount of α-tubulin was equal in all samples. Analysis of the aborted nodules by flow cytometry showed that the downregulation of *ccs52A* correlated with a decrease in nodule ploidy (Figure 5C). Although almost 40% of the cells were endoreduplicated ($>$4C) in the control, only 22% were in the aborted nodules. In the endoreduplicated cell populations, 32C nuclei were dominant (54%) in the control nodules and 8C nuclei were dominant (62%) in the aborted nodules, in which there was a sixfold reduction in the proportion of 32C nuclei and 64C nuclei were not detected. Moreover, because fewer cells entered endoreduplication, the relative proportion of 2C cells increased.

These data demonstrate that the reduced expression of *ccs52A* is linked tightly to a decrease in endoploidy. Moreover, the correlation of reduced ploidy with inefficient nitrogen fixation indicates that endoreduplication cycles do not simply accompany but also play a central role in nodule development.

Aborted Nodules Lack Nodule Zone III and Display Signs of Lytic Events That Result in Cell Death

The structure of the aborted nodule was studied in more detail in stably transformed A4 plants. In wild-type nodules, the meristem (zone I) and the infection zone (zone II) were composed of 6 to 7 and 12 to 14 cell layers, respectively (Figure 6A). In the aborted *ccs52A* antisense nodules, at 15 days after inoculation, no active meristem was found and zone II comprised only four cell layers (Figure 6B), in which bacterial infection and the formation and multiplication of symbiosomes started as in the wild type (cf. Figures 6A and 6B, stars). However, these infected cells did not develop to nitrogen-fixing cells, as in the wild-type nodule zone III (Figure 6A); instead, they were disintegrated rapidly, forming zone IV (Figure 6B). In older cells, rupture of the tonoplast, loss of turgor, and lytic events were observed, resulting in the remnants of infected cells.

To test the impact of downregulated *ccs52A* expression on cell size, the cell surface areas of the 100 largest cells in the aborted nodule sections were measured and compared with those of 100 nitrogen-fixing cells from the control nodules. The average area of nitrogen-fixing cells (1652 $\pm$ 21 μm^2) was 35% larger than that of the cells from the aborted nodules (1217 $\pm$ 21.7 μm^2), indicating that full expression of *ccs52A* is necessary for the development of large symbiotic cells.

Light microscopy studies suggested that bacteroid differentiation in the *ccs52A* antisense nodules might not be accomplished (Figure 6B); this notion was investigated further by electron microscopy. The early and final stages of symbiosome development in wild-type nodules are shown for comparison in

Figures 7A and 7B. The early stage of symbiosome development was comparable in the control nodules (Figure 7A) and in the *ccs52A* antisense nodules (Figure 7C). Each bacterium released from the infection thread was surrounded by a symbiosome membrane and multiplied in the infected cell. In the distal cell layers of zone II, however, a more pronounced aberration of the infected cell ultrastructure was observed (Figures 7D to 7G). As a first step, the bacteroids became more irregular in shape and size. Moreover, significant increase of the peribacteroid space and merging of symbiosomes were detected (Figure 7D, arrows), which were atypical for wild-type *Medicago* nodules. In addition, many small vesicles, probably provacuoles, were formed in the host cytoplasm (Figure 7D, star); these fused occasionally with the symbiosome membranes, forming irregularly shaped structures. In the deeper cell layers, the fusion of multiple symbiosomes and vesicles was more pronounced, and lysis of bacteroids entrapped in these vacuole-like structures was observed as electron-transparent lesions in the bacteroid cytoplasm (Figure 7E). At a more advanced stage, as a result of the autolysis of the symbiosomes, only the "ghosts" of bacteroids remained (Figure 7F). This stage was followed by the degradation or disaggregation of the membrane envelopes and the disruption of all organelles (Figure 7G) and the nucleus, resulting in cell death.

DISCUSSION

In this work, we showed that (1) endoreduplication cycles are required for the development of highly polyploid nitrogen-fixing symbiotic cells, and (2) the cell cycle regulator *ccs52A* is required for nodule differentiation and is a limiting factor for repeated rounds of endoreduplication cycles in which CCS52A may ensure constitutive APC activity.

We reported previously that *ccs52A* expression in fission yeast resulted in mitotic cyclin degradation (Cebolla et al., 1999), confirming that CCS52A, like the orthologous yeast SRW1 and animal CDH1/FZR proteins, was able to interact with the APC and to mediate polyubiquitinylation and the degradation of D box proteins by the 26S proteasome (Harper et al., 2002). The regulated destruction of mitotic cyclins after their function is terminated is essential for cell cycle progression. Alteration of these destruction profiles (e.g., premature degradation of mitotic cyclins) could block cell cycle progression and might be required for cell cycle exit. Unlike animal cells, many differentiated plant cells are arrested in the G2-phase. In *M. truncatula*, the 4C cells are in the majority in most organs (Cebolla et al., 1999; this work). Thus, plant cells might differentiate preferentially via G2 exit. The production of G2-arrested cells by the inactivation of mitotic cyclin-dependent kinase activities, and thus the inhibition of the G2/M transition or the M-phase progression, can be achieved by different mechanisms. The data presented here support the involvement of the APC^{CCS52A} pathway in cell cycle exit and endoreduplication.

In plants, APC can function with several CCS52-related proteins. The Arabidopsis genome contains three *ccs52* and five *cdc20/fzy* genes, each of which encodes a substrate-specific activator of APC that might contribute differentially to cell cycle regulation and the differentiation of various cell types. Based on yeast and animal data, the *cdc20/fzy* genes are expressed in proliferating cells, whereas the *cdh1*-type genes function in both mitotic and postmitotic cells (Harper et al., 2002).

In *M. truncatula*, *ccs52A* was activated and *ccs52B* was repressed during nodule development. In our previous study, we localized the *ccs52A* transcripts in the nodule meristem and in zone II, where endoreduplication cycles occur (Cebolla et al., 1999); however, we did not determine the precise timing of *ccs52A* activation or its involvement in the mitotic and endoreduplication cycles. These questions were addressed in the present work. We showed by the activity of the *ccs52A* promoter–*uidA* fusion, as determined by RT-PCR experiments and protein gel blot analysis, that CCS52A was not produced during the initial mitotic cycles that lead to nodule primordium formation. Therefore, in these cells, other APC activators must ensure the proteolysis of mitotic cyclins or additional APC substrates. Like CCS52A, the *Drosophila* FZR and the chicken CDH1 proteins also are dispensable for cell cycle progression but crucial for cell cycle arrest (Sigrist and Lehner, 1997; Sudo et al., 2001).

The *ccs52A* gene was activated at the final developmental stage of the nodule primordium in the undifferentiated central tissue, and in the differentiated nodules, it was expressed in the meristem and in endoreduplication-competent cells. The activation of *ccs52A* might be controlled by a developmental signal to switch mitotic cells toward differentiation. Such a signal could be the primordium size/number of proliferating cells or the progression of infection threads (or within them the number of bacteria or bacterial products, etc.). The presence of *ccs52A* transcripts in spontaneously formed bacterium-free nodules (A. Cebolla, unpublished data) favors the primordium-size hypothesis, although infection-related signals cannot be excluded during nodulation. Division arrest of cells in the primordium and in the nodule meristem could be the consequence of the APC^{CCS52A}-mediated degradation of mitotic cyclins and other mitotic regulators. With respect to nodule development, two mitotic cyclins, *CycA2;2* and *CycB2;3*, have been studied in *M. sativa* and *M. truncatula*. MedsaCycA2;2, with major activity at the G2/M transition (Roudier et al., 2000), is involved in Nod factor–induced cell proliferation and meristem formation (Roudier et al., 2003), but expression of this gene is repressed in postmitotic cells. Therefore, the CycA2;2 protein is absent in zone II and cannot be a substrate for APC^{CCS52A}. By contrast, *MedsaCycB2;3* (Savouré et al., 1995) is expressed in both the meristem and zone II, where degradation of this cyclin via APC^{CCS52A} might be necessary for M-phase inhibition and for endoreduplication.

In zone II, not only *CycB2;3* and *ccs52A* but many other cell cycle genes as well, including the cyclin-dependent kinase *cdkA*, D-type cyclins, *E2F* transcription factors, and histone H3, remain active (Cebolla et al., 1999; Foucher and Kondorosi, 2000), and the cells are capable of DNA synthesis. During endoreduplication cycles, the alternation of DNA replication with gap periods results in repeated duplication of the genome and the development of polyploid cells up to 32C and 64C. Polyploid nuclei, which contain multiple gene copies and display no condensation of the chromosomes, can have greater gene ex-

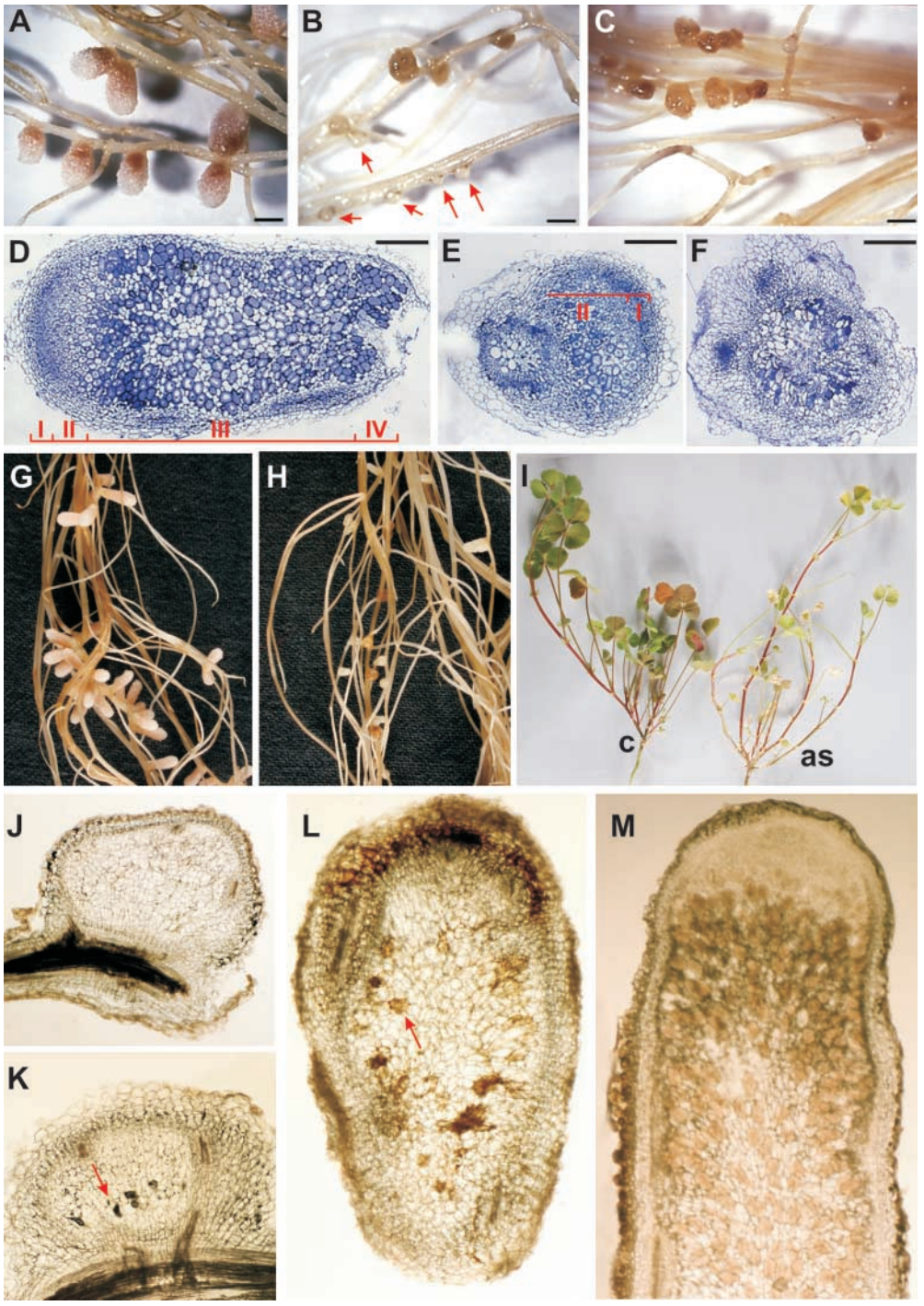

Figure 4. Effect of Reduced *Mtccs52A* Transcript Levels on Nodulation.

(A) to **(F)** Nodules on stable *M. truncatula* transgenic plants transformed with the control vector (**[A]** and **[D]**) and with the *ccs52A* antisense construct (**[B]**, **[C]**, **[E]**, and **[F]**).
(A) Elongated nitrogen-fixing nodules on a control plant. Pink coloration marks nodule zone III.
(B) and **(C)** Healthy primordia (red arrows) and aborted brown nodules on *ccs52A* antisense plant roots at 15 and 25 days after infection, respectively.
(D) Longitudinal section of a control wild-type nodule stained with toluidine blue. The positions of nodule zones I to IV are indicated.
(E) and **(F)** Sections of toluidine blue–stained aborted nodules.
(G) to **(M)** Transgenic hairy-root plants transformed with the control vector (**[G]**, **[I]**, and **[M]**) and the *ccs52A* antisense construct (**[H]** and **[J]** to **[L]**).
(G) Pink nitrogen-fixing nodules on control hairy roots.

pression levels than diploid nuclei. Correspondingly, the intensity of the in situ hybridization signals of the B-type cyclins or histone H3 in zone-II cells increase with ploidy (Cebolla et al., 1999). Because mitotic cyclin production would interfere with endoreduplication, overexpression of cyclin B in these polyploid cells could be compensated for by the proportionally increased activation of *ccs52A* and thus the degradation of the cyclin B proteins. This was not the case in nodules expressing *ccs52A* in the antisense orientation, in which only the expression of cyclin B increased with the ploidy and the *ccs52A* transcript levels remained low. The low level of CCS52A still might be sufficient to compensate for cyclin B overexpression in 4C and 8C cells as they are formed. However, the amount of CCS52A might be insufficient to cope with cyclin B degradation in >8C cells, in which the presence of mitotic cyclins could be incompatible with additional rounds of endocycles. Because these cells did not divide even when mitotic cyclins were produced, the >8C state might have been irreversible, and these cells could not return to the mitotic cycle.

In zone II, which contains cells at different stages of the endoreduplication cycle and at different ploidy levels, the CCS52A protein was localized in the nuclei. During the mitotic cycle, the active hypophosphorylated forms of the orthologous yeast and human Cdh1 proteins were nuclear, whereas, from the onset of S-phase, the inactive hyperphosphorylated form was in the cytoplasm and APC^{Cdh1} activity was periodic (Jaquenoud et al., 2002; Zhou et al., 2003). Although APC activity has not been reported during endoreduplication cycles, nonperiodic APC^{Cdh1} activity in human cells prevented G2 and M events and caused endoreduplication that was linked to the destruction of several mitotic regulators, including cyclin A and cyclin B1 (Sorensen et al., 2000). In agreement with these data, CCS52A displayed abundant nuclear localization throughout zone II, suggesting that CCS52A might activate APC constitutively and that the absence of APC^{CCS52A} periodicity might be indispensable for the endoreduplication cycles. Moreover, the absence of CCS52B in nitrogen-fixing nodules, as well as the restricted activity of the Cdc20 subfamily in proliferating cells (Gieffers et al., 1999), indicated that CCS52A might be the unique activator of APC in symbiotic cells.

We showed that even a low reduction in the *ccs52A* transcript level interfered with nitrogen-fixing nodule development. These nodules displayed significant reduction in the number of endoreduplicated cells, with particular decreases in the proportions of 32C and 64C cells, and they contained more 2C cells than did the wild-type nodules. Rhizobia do not enter diploid cells (Truchet, 1978). As in the antisense nodules, 4C and 8C cells were produced, but they became infected and could not mature to nitrogen-fixing cells. In more severe cases, after primordium formation, the reduced *ccs52A* expression arrested further nodule development and was followed by the rapid extinction of meristematic activity. However, the effect on the meristem cannot be linked directly to *ccs52A*, because CCS52A was dispensable for cell proliferation during primordium formation. CCS52A directs the cells out of the nodule meristem, which has a constant size that is maintained by a dynamic balance of proliferating and nonproliferating cells that leave the meristem. When postmitotic cells are stacked and cannot enter repeated endocycles, they might signal back to the meristem to inhibit the sorting of additional cells. Because cells do not exit the meristem, no new cells are produced and the meristem becomes inactive. This abnormal nodule development might be sensed by the plant, which responds with premature senescence, which also happens in non-nitrogen-fixing alfalfa nodules lacking zone III (Vasse et al., 1990). The brown

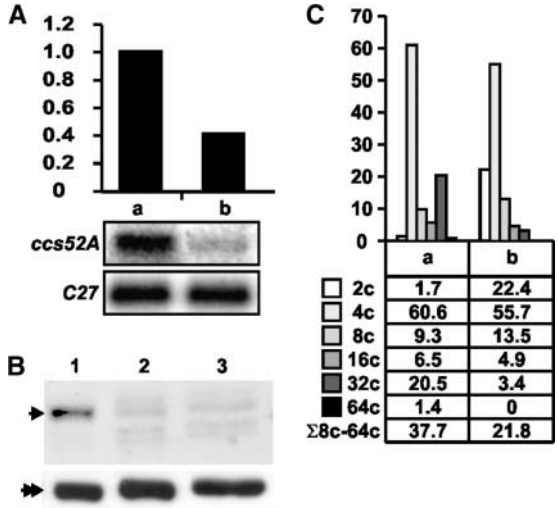

Figure 5. *Mtccs52A* Expression and Ploidy Level Are Reduced in Nodules of *ccs52A* Antisense Transgenic Plants.

(A) RNA gel blot analysis of 10-μg RNA samples from 2-week-old control nodules (a) and aborted nodules from A4 *ccs52A* antisense transgenic plants (b).

(B) Protein gel blot analysis of the CCS52A protein deriving from wild-type nodules (lane 1), globular-stage aborted hairy-root nodules (lane 2), and growing wild-type nodule primordia (lane 3).

(C) Ploidy levels of the (a) and (b) nodules from **(A)**.

Figure 4. (continued).

(H) Aborted nodule development on *ccs52A* antisense hairy roots.

(I) Symptoms of nitrogen starvation in an antisense (as) plant. c, control.

(J) Normal development of the primordium.

(K) Early senescence in a primordium arrested in differentiation (red arrow).

(L) Senescence in the central region of an elongated antisense nodule (red arrow).

(M) Pink nitrogen-fixing cells and the absence of senescence in a control nodule.

Bars = 1 mm in **(A)** to **(C)** and 0.5 mm in **(D)** to **(F)**.

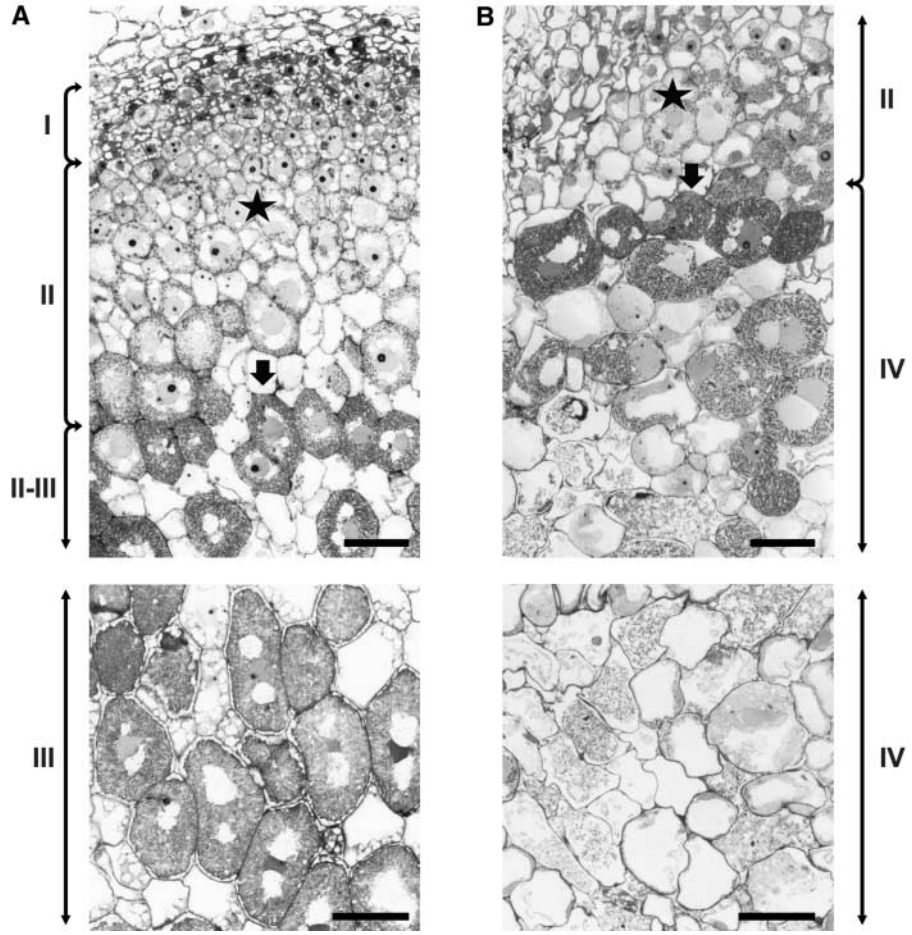

Figure 6. Structure and Differentiation of Plant Cells and Bacteroids in Wild-Type and Aborted Nodules.

(A) Semithin sections of a wild-type nodule at 15 days after inoculation.
(B) Semithin sections of an aborted nodule from a *ccs52A* antisense plant at 15 days after inoculation.
Roman numerals indicates nodule zones. Stars indicate cells at early stages of infection, and arrows indicate cells at more advanced stages of infection and bacteroid differentiation in wild-type and aborted nodules. Bars = 100 μm.

pigmentation caused by the accumulation of secondary metabolites of the phenylpropanoid pathway in the central cells of *ccs52A* antisense nodules is in agreement with these data.

Why are infected nodule cells programmed for endoreduplication? Although endoreduplication is part of most developmental programs in plants, it may have specific functions (Cebolla et al., 1999; Joubes and Chevalier, 2000; Kondorosi et al., 2000). Repeated endoreduplication cycles during symbiotic cell development might have dual roles: (1) to ensure extreme enlargement of cells to host the bacteroids, and (2) to provide energy and nutrient supply for the bacteroids by increased transcriptional and metabolic activities of the host cell. According to our estimations, the volume of the symbiotic cells increases 80-fold compared with that of meristematic cells, and the nitrogen-fixing cells contain ~30,000 to 40,000 bacteroids. Nodules incompetent for efficient nitrogen fixation may contain a few nitrogen-fixing cells that are large and fully packed with bacteroids, but no nodules have been reported with large cells hosting only a few bacteroids. Therefore, bacteroid multiplication and differentiation seem to be coordinated with endoreduplication and the growth of the plant cell. The inhibition of successive endoreduplication cycles by the downregulation of *ccs52A* had a negative effect on cell growth and probably on transcriptional activity, leading to impaired nodule development.

We have shown that *ccs52A* plays a key role in symbiotic cell differentiation and have demonstrated that repeated endoreduplication of these cells is indispensable for nitrogen-fixing nodule development. It remains to be determined how general is the function of *ccs52A* in plant development and how it affects the formation of specific organs, tissues, or cell types. Considering the potential of CCS52A to bind several different proteins, the characterization of these protein partners may elucidate the molecular mechanisms of cell differentiation processes associated with APC^{CCS52} proteolytic pathways.

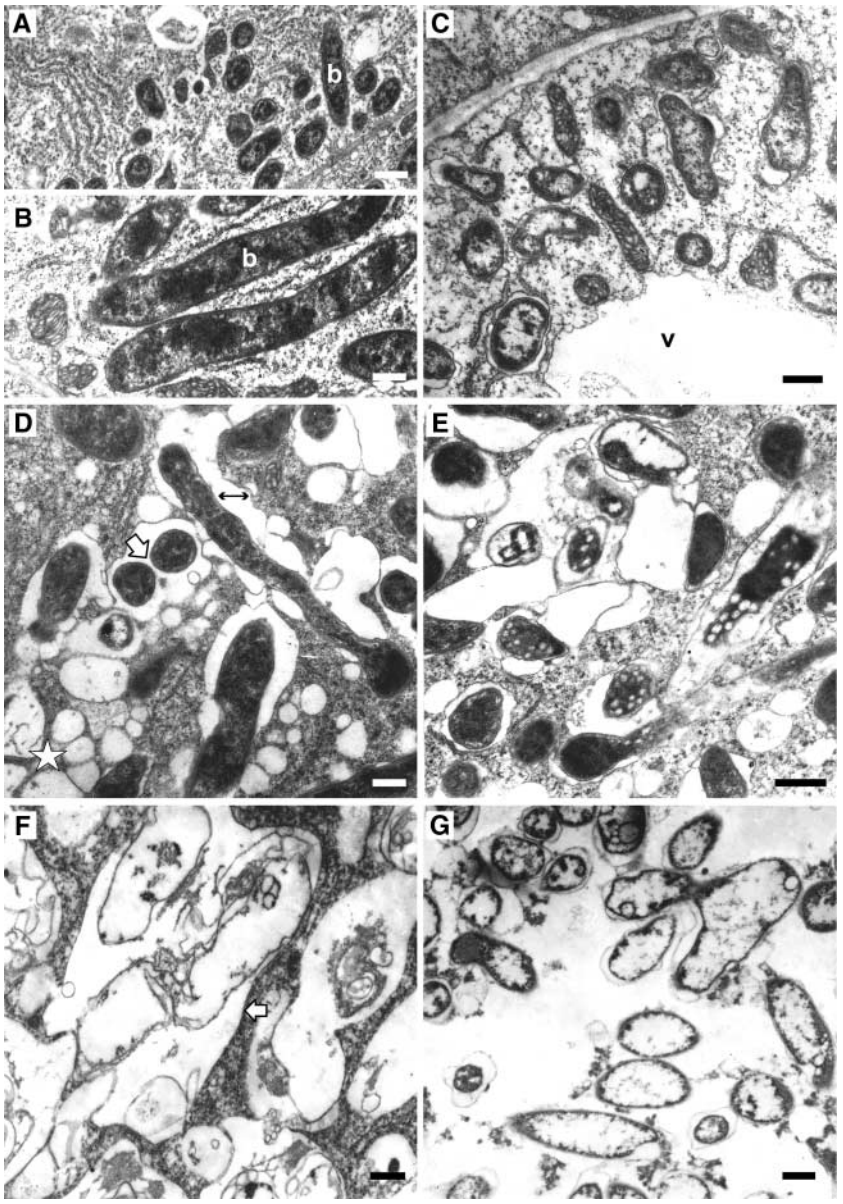

Figure 7. Symbiosome Development and Fate of Bacteroids in Wild-Type and *ccs52A* Antisense Nodule Cells by Electron Microscopy.

(A) and **(B)** Wild-type nodule cells.
(A) Young symbiosomes after release from the infection thread.
(B) Mature symbiosomes representing stage IV (Vasse et al., 1990).
(C) to **(G)** *ccs52A* antisense nodule cells.
(C) Young symbiosomes in the first cell layers of aborted nodules.
(D) Symbiosomes undergoing premature senescence. Note the enlargement of the peribacteroid space (double-headed arrow), the fusion of symbiosomes (white arrow), and the presence of numerous provacuoles (star) that probably fuse later with the symbiosome membrane.
(E) Lysis of symbiosomes entrapped inside vacuole-like structures derived from the fusion of several symbiosomes. Electron-transparent regions in the bacteroid cytoplasm represent the likely sites where autolysis takes place.
(F) Ghost membranes representing the remnants of bacteroids within the still-intact symbiosome membranes (arrow).
(G) The last stage of infected cell senescence, with degradation of host cell cytoplasm.
Bacteroids (b) and vacuoles (v) are indicated. Bars = 200 nm.

METHODS

Molecular Techniques

General molecular biology techniques were used according to Sambrook et al. (1989). The *Mtccs52A* cDNA was isolated from a *Medicago truncatula* R108-1 nodule cDNA library (Györgyey et al., 2000), whereas the genomic region was isolated from a genomic library of *M. truncatula* ecotype Ghor (AF134835; Crespi et al., 1994). The PROMOTER SCAN program (Prestidge, 1995) and the Hamming clustering method (Milanesi et al., 1996) were used for TATA box prediction. Specific primers were P52-GL (5′-TTGGGTTGCTGTGTAGAA-3′) and P52-3end (5′-TAATGCAGGAGAGCACTAT-3′) for *ccs52A* cDNA and c12P1 (5′-GCCACCAATTGAACTCTGTTG-3′) and c12P2 (5′-CAATTTGTAGGTTTACTCGTG-3′) for *ccs52B* cDNA. Reverse transcriptase–mediated (RT) PCR experiments were repeated three times; *Msc27* was amplified by 18 cycles, and *Mtccs52A*, *Mtccs52B*, and *enod40* were amplified by 23 cycles.

Plant Manipulations

Plant growth and nodulation assays were performed according to protocols described online (http://www.isv.cnrs-gif.fr/embo2/manuels/pdf/module1.pdf). Transformation of *M. truncatula* R108-1 with *Agrobacterium tumefaciens* and with *Agrobacterium rhizogenes* was performed according to procedures described online (http://www.isv.cnrs-gif.fr/embo2/manuels/pdf/module2.pdf) that were described originally by Trinh et al. (1998) and Boisson-Dernier et al. (2001), respectively. The *Mtccs52A* promoter–*uidA* transcriptional fusion was constructed by cloning the 2436-bp EcoRI-SmaI promoter region in the binary vector pPR97 (Szabados et al., 1995). For the production of transgenic hairy roots, 40 *M. truncatula* seedlings were transformed with *A. rhizogenes* containing either the *ccs52A* antisense or control construct. After the selection of hairy root–producing plants on agar plates, 18 plantlets of each species were placed in aeroponic factories and grown for 2 weeks in nutrient solution. To elicit nitrogen starvation for nodulation, the medium was changed to a nitrogen-limited nutrient solution for 3 days followed by inoculation of the roots with *Sinorhizobium meliloti* in fresh nitrogen-limited medium.

Histochemical β-glucuronidase (GUS) staining was performed from 2 to 24 h at 37°C as described (Jefferson et al., 1987). For semiquantitative RT-PCR experiments, the roots were spot-inoculated in the nodulation-competent root zone with *S. meliloti* strain 41. RNA was isolated from the nodulation-competent root zone (an ~5-mm root segment) each day after inoculation before nodule primordium became visible and then from the primordia and nodules at successive developmental stages; the nodulation-competent root zone from uninoculated plants was used as a control. The nuclear DNA content of root and nodule materials was measured by flow cytometry (Cebolla et al., 1999) in three independent experiments in which the deviation of the corresponding samples was <10%.

Protein Extraction and Protein Gel Blot Analysis

Rabbit polyclonal anti-CCS52A antiserum was raised against the full-length protein produced in *Escherichia coli* from the pQE32 vector (Qiagen, Valencia, CA) and purified on a Ni column. Protein extracts from nodules were prepared by grinding 50 to 100 mg of nodules in liquid N_2. Frozen powder was suspended in extraction buffer containing 20 mM Hepes, pH 8.2, 150 mM NaCl, 50 mM EDTA, 0.5% Nonidet P-40, 10 mM β-mercaptoethanol, 2 mg/L pepstatin, 2 mg/L leupeptin, 4 mg/L aprotinin, 0.1 mM benzamidine, and 1 mM phenylmethylsulfonyl fluoride and centrifuged at 4°C for 10 min at 16,000*g*. The protein concentration of the supernatant was measured with the Bradford reagent (Bio-Rad). Ten micrograms of protein extracts was separated on an 8% (w/v) polyacrylamide gel and blotted onto a Hybond-P membrane (Amersham Biosciences). Blots were incubated first with a 1:3500 dilution of rabbit anti-MsCCS52A polyclonal antibodies at 4°C for 16 h and then with a 1:30,000 dilution of anti-rabbit IgG–horseradish peroxidase conjugate at room temperature for 1.5 h and developed with an enhanced chemiluminescence kit (Amersham Biosciences). Subsequently, the membranes were reprobed with a 1:2000 dilution of mouse monoclonal anti-α-tubulin clone B-5-1-2 antibody (Sigma) at room temperature for 2 h and with a 1:30,000 dilution of anti-mouse IgG–horseradish peroxidase conjugate secondary antibody at room temperature for 1.5 h to verify the equal loading of proteins.

Immunolocalization, Optical Microscopy, and Electron Microscopy

For immunolocalization, the nodules were fixed for 20 min at 4°C in 4% paraformaldehyde in phosphate buffer, pH 7.2. After three washes in PBS, the nodules were embedded in 6% agarose and cut with a Vibrotome (Micro-cut H1200; Bio-Rad). Sections (35 to 50 μm) blocked with 1% nonfat milk for 30 min were incubated overnight at 4°C with the primary rabbit polyclonal anti-CCS52A antibodies at a 1:30 dilution. Then, the sections were washed in PBS and incubated with the secondary goat anti-rabbit fluorescein isothiocyanate–conjugated antibody (Sigma) at a 1:60 dilution for 1 h at room temperature. Sections were observed with a Polyvar epifluorescence microscope (Reichert-Jung, Nussloch, Germany) and a Sarastro 2000 confocal microscope (Molecular Dynamics, Sunnyvale, CA).

For electron microscopy, the nodules were fixed for 3 h in a mixture of 4% paraformaldehyde and 3% glutaraldehyde in 50 mM potassium phosphate buffer, pH 7.4. The nodules were postfixed with 1% osmium tetroxide and embedded in London Resin White. Ultrathin sections were obtained with an LKB microtome (Stockholm, Sweden) equipped with a glass knife, stained with uranyl acetate and lead citrate, and observed with a Philips EM208 electron microscope (Eindhoven, The Netherlands). Semithin (1 to 2 μm) sections stained with 0.04% toluidine blue were used for optical observations.

Upon request, materials integral to the findings presented in this publication will be made available in a timely manner to all investigators on similar terms for noncommercial research purposes. To obtain materials, please contact E. Kondorosi, eva.kondorosi@isv.cnrs-gif.fr.

ACKNOWLEDGMENTS

We are grateful to S. Brown, O. Catrice, D. Vaubert, and N. Mansion for their help with flow cytometry, transgenic plant cultivation, and photography. J.M.V. and A.C. were supported by the Marie Curie Research Training Grant and Z. Kevei was supported by a PhD Grant of the French (Centre National des Oeuvres Universitaires et Scolaires) and Hungarian governments and by the Jumelage program between the Centre National de la Recherche Scientifique and the Hungarian Academy of Sciences. E.F. was the recipient of a short-term European Molecular Biology Organization fellowship.

Received June 3, 2003; accepted July 14, 2003.

REFERENCES

Boisson-Dernier, A., Chaubaud, M., Garcia, F., Bécard, G., Rosenberg, C., and Barker, D.G. (2001). Hairy roots of *Medicago truncatula* as tools for studying nitrogen-fixing and endomycorrhizal symbiosis. Mol. Plant-Microbe Interact. **14,** 693–700.

Cebolla, A., Vinardell, J.M., Kiss, E., Oláh, B., Roudier, F., Kondorosi,

A., and Kondorosi, E. (1999). The mitotic inhibitor *ccs52* is required for endoreduplication and ploidy-dependent cell enlargement in plants. EMBO J. **18,** 101–109.

Crespi, M.D., Jurkevitch, E., Poiret, M., d'Aubenton-Carafa, Y., Petrovics, G., Kondorosi, E., and Kondorosi, A. (1994). Enod40, a gene expressed during nodule organogenesis, codes for a non-translatable RNA involved in plant growth. EMBO J. **13,** 5099–5112.

Fang, G., Yu, H., and Kirschner, M.W. (1998). Direct binding of CDC20 protein family members activates the anaphase-promoting complex in mitosis and G1. Mol. Cell **2,** 163–171.

Foucher, F., and Kondorosi, E. (2000). Cell cycle regulation in the course of nodule organogenesis in *Medicago*. Plant Mol. Biol. **43,** 773–786.

Galitski, T., Saldanha, A.J., Styles, C.A., Lander, E.S., and Fink, G.R. (1999). Ploidy regulation of gene expression. Science **285,** 251–254.

Genschik, P., Criqui, M.C., Parmentier, Y., Derevier, A., and Fleck, J. (1998). Cell cycle–dependent proteolysis in plants: Identification of the destruction box pathway and metaphase arrest produced by the proteasome inhibitor MG132. Plant Cell **10,** 2063–2076.

Gieffers, C., Peters, B.H., Kramer, E.R., Dotti, C.G., and Peters, J.-M. (1999). Expression of the CDH1-associated form of the anaphase-promoting complex in postmitotic neurons. Proc. Natl. Acad. Sci. USA **96,** 11317–11322.

Glotzer, M., Murray, A.W., and Kirschner, M.W. (1991). Cyclin is degraded by the ubiquitin pathway. Nature **349,** 132–138.

Györgyey, J., Gartner, A., Németh, K., Magyar, Z., Hirt, H., Heberle-Bors, E., and Dudits, D. (1991). Alfalfa heat shock genes are differentially expressed during somatic embryogenesis. Plant Mol. Biol. **16,** 999–1007.

Györgyey, J., Vaubert, D., Jiménez-Zurdo, J.I., Charon, C., Troussard, L., Kondorosi, A., and Kondorosi, E. (2000). Analysis of *Medicago truncatula* nodule expressed sequence tags. Mol. Plant-Microbe Interact. **13,** 62–71.

Harper, J.W., Burton, J.L., and Solomon, M.J. (2002). The anaphase-promoting complex: It's not just for mitosis any more. Genes Dev. **16,** 2179–2206.

Jaquenoud, M., van Drogen, F., and Peter, M. (2002). Cell cycle-dependent nuclear export of Cdh1p may contribute to the inactivation of APC/Ccdh1. EMBO J. **21,** 6515–6526.

Jefferson, R.A., Kavanagh, T.A., and Bevan, M.W. (1987). GUS fusions: β-Glucuronidase as a sensitive and versatile gene fusion marker in higher plants. EMBO J. **6,** 3901–3907.

Joubes, J., and Chevalier, C. (2000). Endoreduplication in higher plants. Plant Mol. Biol. **43,** 735–745.

Kondorosi, E., Roudier, F., and Gendreau, E. (2000). Plant cell-size control: Growing by ploidy? Curr. Opin. Plant Biol. **3,** 488–492.

Littlepage, L.E., and Ruderman, J.V. (2002). Identification of a new APC/C recognition domain, the A box, which is required for the Cdh1-dependent destruction of the kinase Aurora-A during mitotic exit. Genes Dev. **16,** 2274–2285.

Milanesi, L., Muselli, M., and Arrigo, P. (1996). Hamming clustering method for signals prediction in 5′ and 3′ regions of eukaryotic genes. Comput. Appl. Biosci. **12,** 399–404.

Nagl, W. (1978). Endopolyploidy and Polyteny in Differentiation and Evolution. (Amsterdam: North-Holland Publishing).

Pfleger, C.M., and Kirschner, M.W. (2000). The KEN box: An APC recognition signal distinct from the D box targeted by Cdh1. Genes Dev. **14,** 655–665.

Pfleger, C.M., Lee, E., and Kirschner, M.W. (2001). Substrate recognition by the Cdc20 and Cdh1 components of the anaphase-promoting complex. Genes Dev. **15,** 2396–2407.

Prestidge, D.S. (1995). Predicting Pol II promoter sequences using transcription factor binding sites. J. Mol. Biol. **249,** 923–932.

Roudier, F., Fedorova, E., Györgyey, J., Fehér, A., Brown, S., Kondorosi, A., and Kondorosi, E. (2000). Cell cycle function of a *Medicago sativa* A2-type cyclin interacting with a PSTAIRE-type cyclin-dependent kinase and a retinoblastoma protein. Plant J. **23,** 73–83.

Roudier, F., Fedorova, E., Lebris, M., Lecomte, P., Györgyey, J., Vaubert, D., Horvath, G., Abad, P., Kondorosi, A., and Kondorosi, E. (2003). The Medicago species A2-type cyclin is auxin regulated and involved in meristem formation but dispensable for endoreduplication-associated developmental programs. Plant Physiol. **131,** 1091–1103.

Sambrook, J., Fritsch, E.F., and Maniatis, T.A. (1989). Molecular Cloning: A Laboratory Manual, 2nd ed. (Cold Spring Harbor, NY: Cold Spring Harbor Laboratory Press).

Savouré, A., Feher, A., Kalo, P., Petrovics, G., Csanàdi, G., Szécsi, J., Kiss, G., Brown, S., Kondorosi, A., and Kondorosi, E. (1995). Isolation of a full length mitotic cyclin cDNA clone CycIIIMs from *Medicago sativa*: Chromosomal mapping and expression. Plant Mol. Biol., **27,** 1059–1070.

Sigrist, S.J., and Lehner, C.F. (1997). *Drosophila* fizzy-related down-regulates mitotic cyclins and is required for cell proliferation arrest and entry into endocycles. Cell **90,** 671–681.

Sorensen, C.S., Lukas, C., Kramer, E.R., Peters, J.M., Bartek, J., and Lukas, J. (2000). Nonperiodic activity of the human anaphase-promoting complex-Cdh1 ubiquitin ligase results in continuous DNA synthesis uncoupled from mitosis. Mol. Cell. Biol. **20,** 7613–7623.

Sudo, T., Ota, Y., Kotani, S., Nakao, M., Takami, Y., Takeda, S., and Saya, H. (2001). Activation of Cdh1-dependent APC is required for G1 cell cycle arrest and DNA damage-induced G2 checkpoint in vertebrate cells. EMBO J. **20,** 6499–6508.

Szabados, L., Charrier, B., Kondorosi, A., de Bruijn, F.J., and Ratet, P. (1995). New plant promoter and enhancer testing vectors. Mol. Breed. **1,** 419–423.

Trinh, T.H., Ratet, P., Kondorosi, E., Durand, P., Kamaté, K., Brown, S., Bauer, P., and Kondorosi, A. (1998). Simple, rapid and efficient transformation of diploid *Medicago truncatula* and *Medicago falcata* lines improved for somatic embryogenesis. Plant Cell Rep. **17,** 345–355.

Truchet, G. (1978). Sur l'état diploide des cellules du méritème des nodules radiculaires des légumineuses. Ann. Sci. Nat. Bot. Paris **19,** 3–38.

Vandepoele, K., Raes, J., De Veylder, L., Rouzé, P., Rombauts, S., and Inzé, D. (2002). Genome-wide analysis of core cell cycle genes in Arabidopsis. Plant Cell **14,** 903–916.

Vasse, J., de Billy, F., Camut, S., and Truchet, G. (1990). Correlation between ultrastructural differentiation of bacteroids and nitrogen fixation in alfalfa nodules. J. Bacteriol. **172,** 4295–4306.

Visintin, R., Prinz, S., and Amon, A. (1997). CDC20 and CDH1: A family of substrate-specific activators of APC-dependent proteolysis. Science **278,** 460–463.

Vodermaier, H.C. (2001). Cell cycle: Waiters serving the destruction machinery. Curr. Biol. **11,** R834–R837.

Zachariae, W., Schwab, M., Nasmyth, K., and Seufert, W. (1998). Control of cyclin ubiquitination by CDK-regulated binding of Hct1 to the anaphase promoting complex. Science **282,** 1721–1724.

Zhou, Y., Ching, Y.-P., Chun, A.C.S., and Jin, D.-Y. (2003). Nuclear localization of the cell cycle regulator CDH1 and its regulation by phosphorylation. J. Biol. Chem. **278,** 12530–12536.